Predictive Control of Voltage and Current in a Fuel Cell–Ultracapacitor Hybrid

Wes Greenwell and Ardalan Vahidi, *Member, IEEE*

***Abstract*—This paper presents a system integration and control strategy for managing power transients on a Nexa polymer electrolyte membrane fuel cell (FC) with the assistance of an ultracapacitor (UC) module. The two degrees of freedom provided by the use of two dc/dc converters enable the independent low-level control of dc bus voltage and the current split between the FC and UC. The supervisory-level control objectives are to respond to rapid variations in load while minimizing damaging fluctuations in FC current and maintaining the UC charge (or voltage) within allowable bounds. The use of a model predictive control approach which optimally balances the distribution of power between the FC and UC while satisfying the constraints is shown to be an effective method for meeting the supervisory-level objectives. The results are confirmed in experiments.**

***Index Terms*—Energy management, fuel cell, model predictive control, ultracapacitor.**

I. Introduction

A FUEL CELL (FC)–ULTRACAPACITOR (UC) hybrid combines the high energy density of hydrogen FC with the high power density of UC, resulting in a system with improved performance and reduced size [1], [2]. Due to the limited response rate of its reactant supply, a proton exchange membrane FC is limited in following fast transients in power demand [3], [4]. Supplementing the FC with an energy storage device, which can provide the needed power during quick power transients, results in an improved load-following capability. Moreover, the lifetime of the FC stack is improved by reducing the large transients that the stack must provide [5]–[7]. In such a hybrid system, the FC can be sized to meet the expected power demand at steady state [8], [9], and the energy storage device is sized to buffer the power transients.

In the hybrid setup considered in this paper, the power transients can be effectively met by a compact UC module. While power density and efficiency of lithium ion batteries have improved considerably in recent years [10], their cost is still too high on a power basis (in dollars per kilowatt), their performance degrades at low temperature and with aging, and deep discharge cycles would negatively influence their life [11]. The cycle life of lithium ion batteries is now close to meeting the target expectations, but their calender life is still short of requirements [11]. Unlike batteries, which store and release energy through chemical reactions, UCs store energy electrostatically and have very low internal resistance [12]. This results in very fast charge/discharge rates with very little power loss and overall charge/discharge efficiencies of greater than 95% [11]. In [13], it is shown that, for the same performance, UCs are more cost effective than lithium ion auxiliary storage in an FC vehicle. Long calender life, as well as cycle life [14], robust performance at low temperatures, and lower cost on a power basis [11] make a UC module a better choice than lithium ion batteries in the hybrid system considered in this paper.

While large current transients on the FC can be filtered by simply connecting the UC to the FC in parallel [15], such a configuration will not provide the required degrees of freedom for actively managing the bus voltage and the power split decision. For more control authority, the addition of one or more power electronic devices is necessary. Possible configurations are several [16], each with its own advantages and disadvantages. In this paper, to achieve full control authority over dc bus voltage and FC and UC current, the use of two power electronic devices is proposed. A dc/dc converter in voltage-control mode will regulate the bus voltage, and another dc/dc converter operated in current-control mode enables active control of FC and UC currents. The power split ratio is determined by a supervisory controller which plays critical roles in improved load-following, the reduction of losses, and increased lifetime. In the literature, a number of control methods have been proposed for meeting similar objectives. Many use a rule-based supervisory controller at the high-level and simple filters [17], [18] or proportional–integral–derivative (PID) loops [19], [20] at low level. Sciarretta *et al.* [21] have demonstrated the effectiveness of an equivalent consumption minimization strategy, which determines optimal control actions based on a cost function quantifying the instantaneous cost of electrical and fuel energy. For FC–UC hybrids, energy management based on fuzzy logic [2] and neural networks [22] has also been proposed. Optimal control methods, such as unconstrained optimal control [7], dynamic programming [23], [24], and model predictive control (MPC) [25], have been proposed in the past.

In this paper, we investigate two control methods: 1) a rule-based method and 2) an MPC approach for the power management of a UC–FC hybrid. The control objectives are as follows: 1) to minimize the current transients seen by the FC; 2) to follow the demand power as closely as possible; and 3) to prevent overcharge or overdischarge of the UCs. We describe

Manuscript received February 27, 2009; revised May 18, 2009 and June 24, 2009; accepted August 7, 2009. Date of publication September 18, 2009; date of current version May 12, 2010. An earlier version of this paper was published in the Proceedings of the 2008 American Society of Mechanical Engineers Dynamic Systems and Control Conference [40].

W. Greenwell was with the Department of Mechanical Engineering, Clemson University, Clemson, SC 29634 USA. He is now with Michelin Americas Research, Greenville, SC 29605-6131 USA (e-mail: wgreenw@clemson.edu).

A. Vahidi is with the Department of Mechanical Engineering, Clemson University, Clemson, SC 29634 USA (e-mail: avahidi@clemson.edu).

Color versions of one or more of the figures in this paper are available online at http://ieeexplore.ieee.org.

Digital Object Identifier 10.1109/TIE.2009.2031663

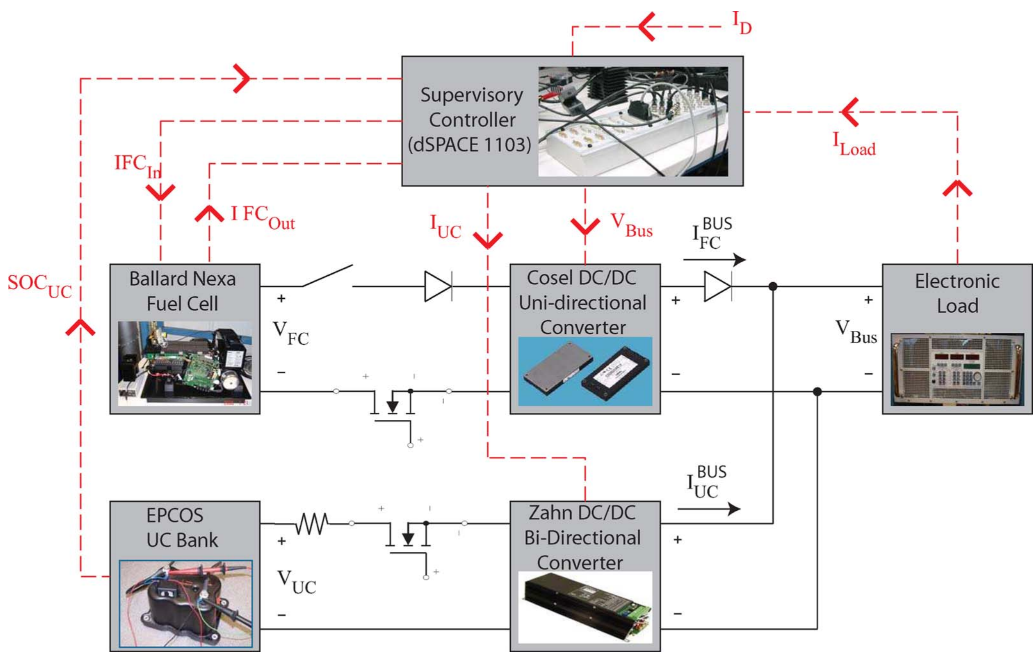

Fig. 1. FC/UC hybrid system schematic.

the system architecture, the power electronic devices used, their specification, and their interface to the supervisory-level control system. These details are core to a successful implementation but often not clearly described in the existing literature on the integration of FC and UCs. In [26], the advantages of MPC for the power management of an FC and UC hybrid are discussed, but only simulation results are presented. More recently, several publications have highlighted the advantages and implementation of MPC for electric machines. Specifically, MPC has been proposed for the control of ac machines [27], [28], motor torque control [29], [30], switch mode power supplies [31], and power converters [32]–[35]. To the best of our knowledge, the feasibility of an MPC approach for the *energy management* of hybrid power systems has not been experimentally shown before. This paper fills this gap by providing details on the hardware employed, system integration and architecture, and real-time implementation of an advanced energy management strategy.

This paper is organized as follows: First, the setup of the hybrid test stand is discussed, and testing procedures are explained. Next, the control problem is formulated, and the real-time implementation of the control strategy is explained. The simulation and experimental results are then discussed. Finally, conclusions are drawn based on the controller/system performance in meeting its objectives.

II. Experimental Setup

The hybrid power system considered in this paper consists of an FC and a UC bank connected in parallel. An electronic load is used to draw requested amounts of power from the hybrid system. A real-time controller board is used to provide supervisory control over the system by determining the portion of the power demand met by the FC (energy supply) and UC bank (energy storage). The controller implements these control actions through power electronic devices, which are used to regulate and condition the voltage and current of the FC and UC. Fig. 1 shows a general schematic of the hybrid power system.

The FC used in this setup is a Ballard Nexa FC module. The Nexa FC stack uses pure gaseous hydrogen as fuel to produce unregulated dc power. The module has an onboard blower which pumps air into the stack, where the oxygen is used to complete the chemical reaction. Stack temperature is maintained through the use of a cooling fan, and an integrated humidifier ensures that the humidity of the stack stays within a desirable operating region. This stand-alone module has a controller which implements all control actions necessary for the continued operation of the stack (hydrogen valves, compressor, cooling fan, etc). The module also has emergency shutoff provisions that shut down the stack when hazardous conditions are perceived. Some of the module output specifications are as follows:

1) peak power: 1200 W;
2) voltage at rated power: 26 VDC;
3) current at rated power: 42 A;
4) output voltage range: 22–50 VDC.

The FC output is unregulated, meaning that the stack voltage drops as the current it provides is increased. Therefore, a power electronic device is required to maintain a steady bus voltage. Three Cosel *CDS*6002428 forward converters are connected in parallel in order to regulate the FC output. The parallel association of the converters has a rated power of 1800 W and maintains a bus voltage of 24 VDC over the entire voltage range supplied by the FC module. The FC and dc/dc converter combination or the energy supply side of the hybrid system is shown in Fig. 2.

A single EPCOS UC module is connected in parallel with the dc link via a dc/dc converter to act as a power buffer and provide energy storage. The module specifications are as follows:

1) capacitance: 200 F;
2) max rated voltage: 14 V;

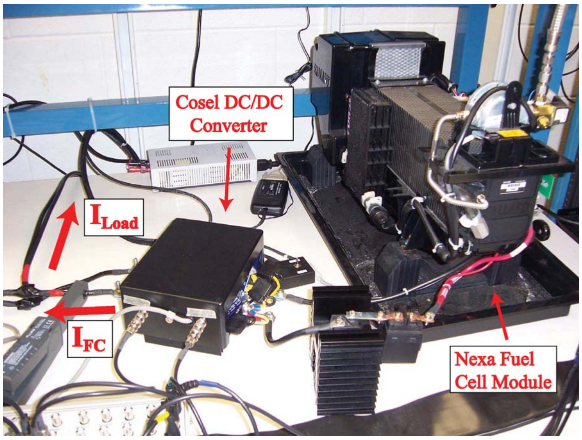

Fig. 2. Energy supply side of hybrid system.

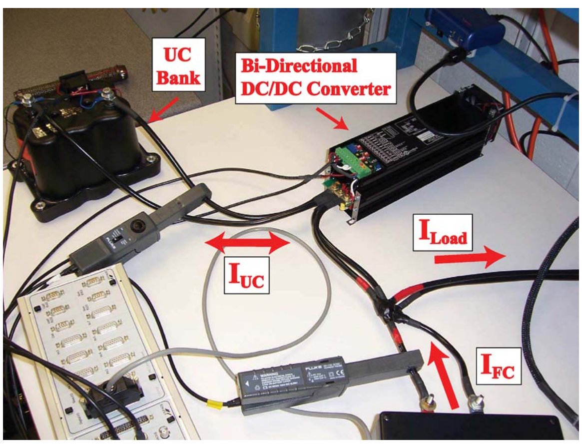

Fig. 3. Energy storage side of hybrid system.

3) energy storage: 5.44 Wh;
4) peak power delivery: 4000 W.

A Zahn *DC*5050-*SU* dc/dc converter is used to regulate the power delivered by the UC bank to the bus. This half-bridge converter has bidirectional current-control capabilities. The acceptable input voltage range is 12–42 VDC, and the maximum output power is 1200 W. The converter can be internally powered by either the UC or the FC, so that the operation does not shut down as the UC voltage drops. The UC bank and dc/dc converter combination or the energy storage side of the hybrid system is shown in Fig. 3.

The FC and UC bank converters work together in order to maintain a constant bus voltage and control the current delivered by each source. The FC converter operates in a voltage-control mode to maintain the bus voltage, and the UC bank converter operates in a current-control mode to provide supplemental current to the electronic load.

The control strategy that controls the bus voltage and current split between the FC and UC is implemented using a dSPACE *ds*1103 controller. The controller is first built in Simulink; MATLAB's real-time workshop is then used to generate C-code for the target processor. The UC voltage is sensed by voltage probes, and the FC and UC currents are measured using current clamps. The current measurement is filtered using a linear first-order low-pass filter. The dc/dc converters are used as actuators to enforce the high-level control decisions. A simple PI control loop in the Zahn dc/dc converter ensures offset-free tracking of the current reference issued to it by the higher level power management strategy. The details of the supervisory power management scheme are described in the next section. The combined system allows precise control of current delivery (at constant bus voltage) to the load from the hybrid system.

III. Control Problem Formulation

The control objective is to meet the power demand while minimizing FC power fluctuations, which helps extend FC life. The FC converter maintains the bus voltage constant (at 24 V); thus, the problem of meeting the power demand is simplified from a power split problem to a current split problem. In other words, it is required that I_{BUS} defined as

$$I_{\mathrm{BUS}} = I_{\mathrm{FC}}^{\mathrm{BUS}} + I_{\mathrm{UC}}^{\mathrm{BUS}} \tag{1}$$

is always equal to the total current demand I_D. Here, $I_{\mathrm{UC}}^{\mathrm{BUS}}$ and $I_{\mathrm{FC}}^{\mathrm{BUS}}$ are the currents delivered to the bus by the UC and FC, respectively; positive UC current $(I_{\mathrm{UC}}^{\mathrm{BUS}} > 0)$ represents the UC discharge. By maintaining the bus voltage with the FC dc/dc converter, the UC dc/dc converter provides an extra degree of freedom for controlling the current split. The current demand (I_D) is a measured variable; thus, by controlling $I_{\mathrm{UC}}^{\mathrm{BUS}}$, the amount of current drawn from the FC can be determined.

To extend the FC lifetime and improve fuel economy, it is desirable to minimize the transients seen by the FC. Therefore, ideally, we like to run the FC at a constant operating point and have the UC module absorb any change in current.

The relationship between the Nexa FC module output power and efficiency was determined experimentally. This relates the amount of power generated by the FC (as measured at the output terminals) to the theoretical power based on the hydrogen fuel's energy content and flow rate. The results show that the FC efficiency is inversely proportional to the amount of power delivered. However, the converter used to regulate the FC to a constant bus voltage has a higher input/output efficiency at high power. Fig. 4 shows how the FC and dc/dc converter, when connected, result in a combined efficiency with a peak. This peak, which represents the operating point for maximum fuel economy, occurs at an FC bus current of 20 A (assuming 24-V bus). We refer to this current as the FC ideal operating current in the rest of this paper and represent it by $I_{\mathrm{FC}}^{\mathrm{OP}}$.

The current that the UC bank is capable of delivering depends on its state of charge (SOC). The SOC is simply defined as the UC voltage over its maximum rated voltage and ranges from zero at no charge to one at full charge. The SOC of the UC bank becomes a key parameter when determining the current split between the two power supplies. One of the control objectives is to enforce upper and lower bounds on the UC SOC at all times.

In our proposed architecture, the charge and discharge of the UC are controlled by a bidirectional dc/dc converter. Assuming that the UC line resistance is negligible, the relationship between the UC currents before and after the converter (I_{UC}

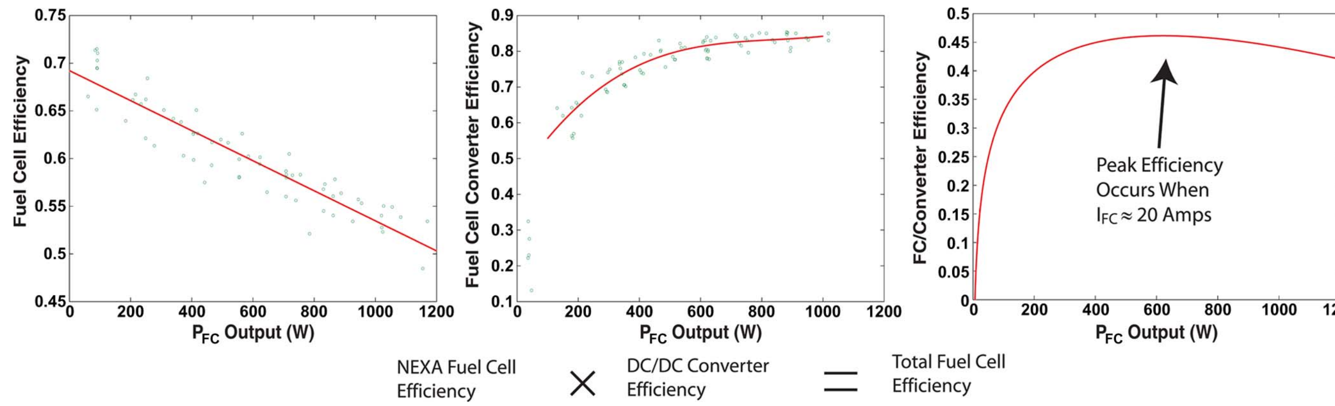

Fig. 4. FC/converter combined efficiency.

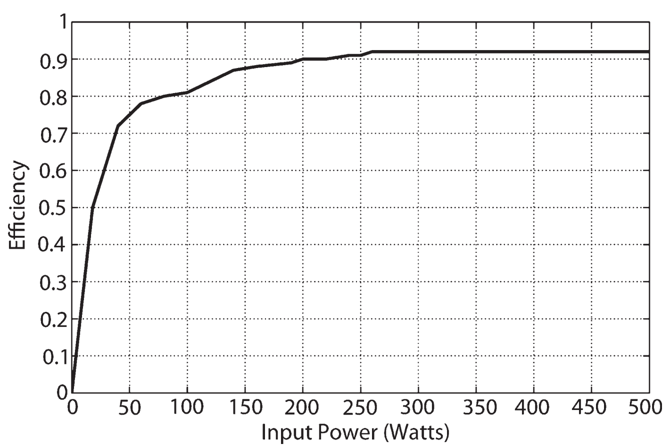

Fig. 5. Bidirectional dc/dc converter efficiency map.

and $I_{\mathrm{UC}}^{\mathrm{BUS}}$, respectively) is determined using the conservation of power

$$\beta \cdot I_{\mathrm{UC}} \cdot V_{\mathrm{UC}} = V_{\mathrm{BUS}} \cdot I_{\mathrm{UC}}^{\mathrm{BUS}} \tag{2}$$

$$\beta = \begin{cases} \eta_{\mathrm{discharge}}, & \text{while discharging} \\ 1/\eta_{\mathrm{charge}}, & \text{while charging} \end{cases} \tag{3}$$

where V_{UC} is the voltage of the UC, V_{BUS} is the bus voltage, and η_{charge} and $\eta_{\mathrm{discharge}}$ are the charge and discharge efficiencies. The relationship between the converter input power and the converter efficiency η is shown in Fig. 5, where the input power is from the bus when charging and from the UC bank when discharging.

When given the current demand I_D and the UC SOC, a converter efficiency map can be used to determine the current which is needed from the UC ($I_{\mathrm{UC}}^{\mathrm{OP}}$) in order for the FC to provide its ideal operating current ($I_{\mathrm{FC}}^{\mathrm{OP}}$). Therefore, when $I_{\mathrm{FC}}^{\mathrm{OP}}$ is specified, and I_D and SOC are measured, $I_{\mathrm{UC}}^{\mathrm{OP}}$ can be determined

$$I_{\mathrm{UC}}^{\mathrm{OP}} = \frac{V_{\mathrm{BUS}}\left(I_D - I_{\mathrm{FC}}^{\mathrm{OP}}\right)}{\beta \cdot V_{\mathrm{MAX}} \cdot \mathrm{SOC}} \tag{4}$$

where V_{MAX} is the UC voltage at full charge.

A. Rule-Based Power Management Strategy

First, a simple rule-based algorithm was devised, which determines the UC current, based on the current demand and the SOC of UC. The FC supplies the difference between the current demand and the current supplied by the UC.

The current demand, FC operating current, and SOC of the UC are used along with (4) in order to find $I_{\mathrm{UC}}^{\mathrm{OP}}$ or the current required by the UC in order for the FC to provide its operating current. This value is then passed through a first-order filter $H(s)$ to determine the desired current out of UC I_{UC}^{D}

$$\frac{I_{\mathrm{UC}}^{D}}{I_{\mathrm{UC}}^{\mathrm{OP}}} = H(s) = \frac{\tau \cdot s}{\tau \cdot s + 1} \tag{5}$$

where τ is the time constant of the filter. This first-order filter assures that the current delivered by the FC always approaches the current demand at steady state. This is important because the UC bank should only be considered a storage device for buffering large transients and not as a source to provide or absorb energy for continuous periods. The speed at which the FC current approaches the demand can be adjusted by the filter parameter τ.

To respect the bounds on the SOC of UC, the desired UC current is adjusted by a gain $K \in [0\ 1]$, which is a function of SOC, as shown in Fig. 6; i.e.,

$$I_{\mathrm{UC}}(t) = K \cdot I_{\mathrm{UC}}^{D}(t) \tag{6}$$

where I_{UC} is the actual current that the UC should supply. When SOC is far from reaching a constraint, K is set equal to one, and all the desired UC currents are used; however, when SOC is approaching a constraint, the gain is decreased as a quadratic function of SOC until $K = 0$, i.e.,

$$K = 1 - 25(\mathrm{SOC} - 0.7)^2.$$

This quadratic form penalizes large deviations from the desired SOC of 0.7, more aggressively than a linear form. When the SOC reaches its limits, K is set to zero so that no current is taken from UC. The resulting controller is *ad hoc* but provides a simple power management strategy to meet the current demanded while considering various low-level objectives and constraints, such as SOC violations.

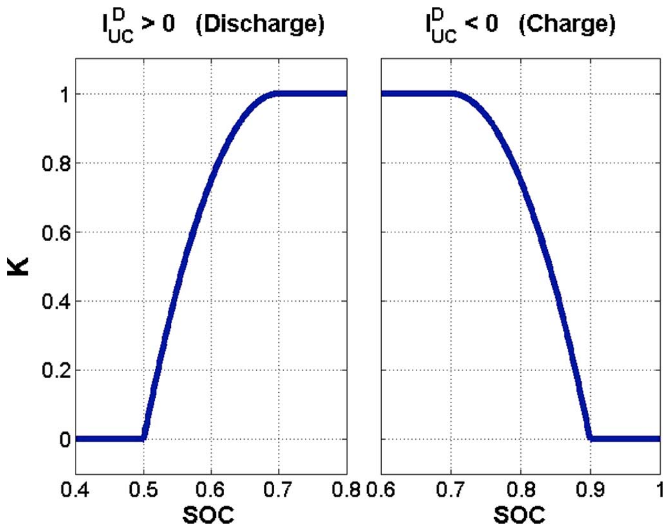

Fig. 6. SOC penalty factor K.

It should be noted that, due to use of a high-pass filter in determining the UC's current, the UC current will decay to zero at steady state. This will prevent the UC's charge recovery and peak load shaving at steady state. To allow active charging of the UC at steady state, an "active recharge mode" was programmed into the rule-based controller. In this mode, the FC will slowly increase its current output in order to charge the UC bank back to the desired SOC of 0.7.

The performance of the rule-based controller was tested on the real-time platform, and the results will be discussed in a later section.

B. Model Predictive Power Management Strategy

The rule-based scheme works based on instantaneous current demand and SOC of the UC. Smoother power split decisions are expected if a predictive planning strategy is employed. In [25] and [26], the merits of an MPC strategy in the power management of an FC/UC hybrid are demonstrated via simulations. In this paper, the performance and the viability of implementing an MPC power management strategy are evaluated in real-time experiments.

MPC is a model-based control approach that utilizes a model of the system to project the future response as a function of control inputs and known disturbances; it then determines the optimal control inputs by minimizing a performance index over a finite prediction horizon. Pointwise-in-time constraints on the inputs, outputs, and states can be explicitly enforced in the optimization. The first control input from the calculated sequence of optimal inputs is applied to the system, and the optimization process is repeated at every time step in a receding horizon fashion. When the model and constraints are linear and the performance index is a quadratic function of the states and the inputs, the MPC problem can be cast as a quadratic programming problem for which efficient solutions exist [36]–[38].

The predictive nature of MPC allows preemptive action to be taken if the system is approaching a constraint. This makes MPC a good candidate for the FC–UC power management problem because of the objective of reducing sharp transients in the FC current while invoking the constraints on the UC's SOC. Moreover, unlike the heuristic tuning in rule-based method, the MPC strategy can be tuned more systematically by adjusting the penalty weights in the performance index.

In developing a dynamic model for the MPC design, only the dynamics of the UC's SOC is considered. Unlike in [25] and [26], where explicit control of FC internal states was sought, in this paper, the main criterion is controlling the current taken from the FC; therefore, the dynamics of the internal states of the FC are not considered. The dynamics of power electronic devices are very fast and thus neglected. The rate of change of SOC of the UC is

$$\frac{d}{dt}\mathrm{SOC} = \frac{-I_{\mathrm{UC}}}{C \cdot V_{\mathrm{MAX}}}. \tag{7}$$

A cost function is formed

$$J = \sum_{i=k}^{k+P} \Big(W_1 \left(\mathrm{SOC}(i|k) - \mathrm{SOC}^{\mathrm{OP}}(i) \right)^2 + W_2 \left(I_{\mathrm{UC}}(i|k) - I_{\mathrm{UC}}^{\mathrm{OP}}(i) \right)^2 \Big) \tag{8}$$

which penalizes the following: 1) deviations from FC operating point 2) deviations in SOC, with penalty weights W_i. Here, SOC$(i|k)$ represents the SOC predicted at the current time step k for the ith step in the future using the model of the system. We also enforce bounds on UC SOC

$$0.5 \leq \mathrm{SOC} \leq 0.9$$

as a hard constraint in the optimization process. Because the relationship between the UC voltage and its SOC is linear, enforcing $(0.5 \leq \mathrm{SOC} \leq 0.9)$ is equivalent to enforcing the constraint $0.5V_{\max} \leq V_{\mathrm{UC}} \leq 0.9V_{\max}$ on the UC voltage. Our rational for using a lower bound of 0.5 on the SOC was the fact that a UC releases 75% of its stored energy when discharged from full charge to SOC $= 0.5$. Below that level, only 25% of the energy is available, but the voltage will be low for the dc/dc converter that we have in the lab. That is, the voltage drops below what the Zahn dc/dc converter can accept. An upper constraint of 0.9 is just a margin against overcharging the UC which could be harmful to it.

The cost function (8) subject to the model equation (7) and inequality constraints on SOC is minimized at each sample time to determine the sequence of the next $N \leqslant P$ control inputs $U_i(k) = [u(k) \quad u(k+1) \quad \cdots \quad u(k+N-1)]$ over the future horizon P. When $N < P$, the remaining control moves $[u(k+N) \quad u(k+N+1) \quad \cdots \quad u(k+P-1)]$ are assumed to be zero. Here, the control input u (also called manipulated variable) is the UC current I_{UC}. According to the standard MPC design, only the first entry of the control sequence $U_i(k)$ is applied to the system, the optimization horizon is moved one step forward, the model and constraints are updated if necessary, and the optimization process is repeated to obtain the next optimal control sequence $U_i(k+1)$. With a linear model of the process and linear constraints and the quadratic cost in (8), this dynamic optimization problem can be cast as quadratic program for which efficient real-time solutions exist [36]–[38].

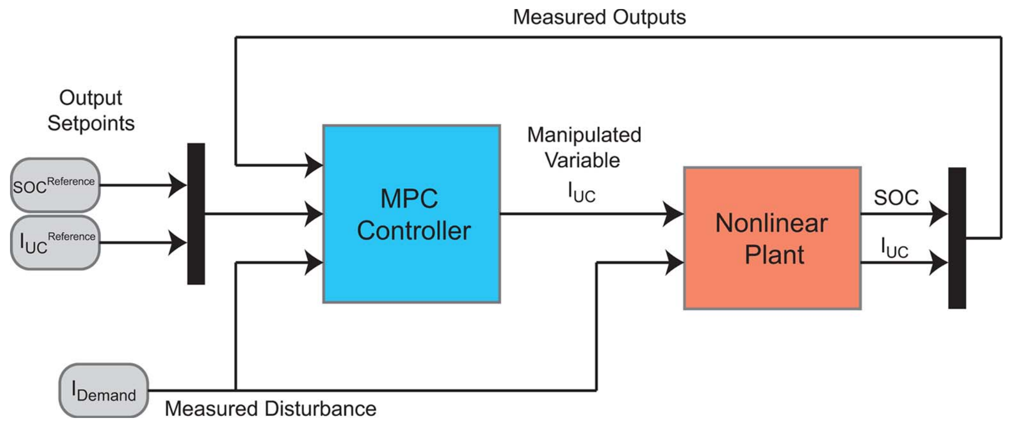

Fig. 7. Block diagram of MPC controller.

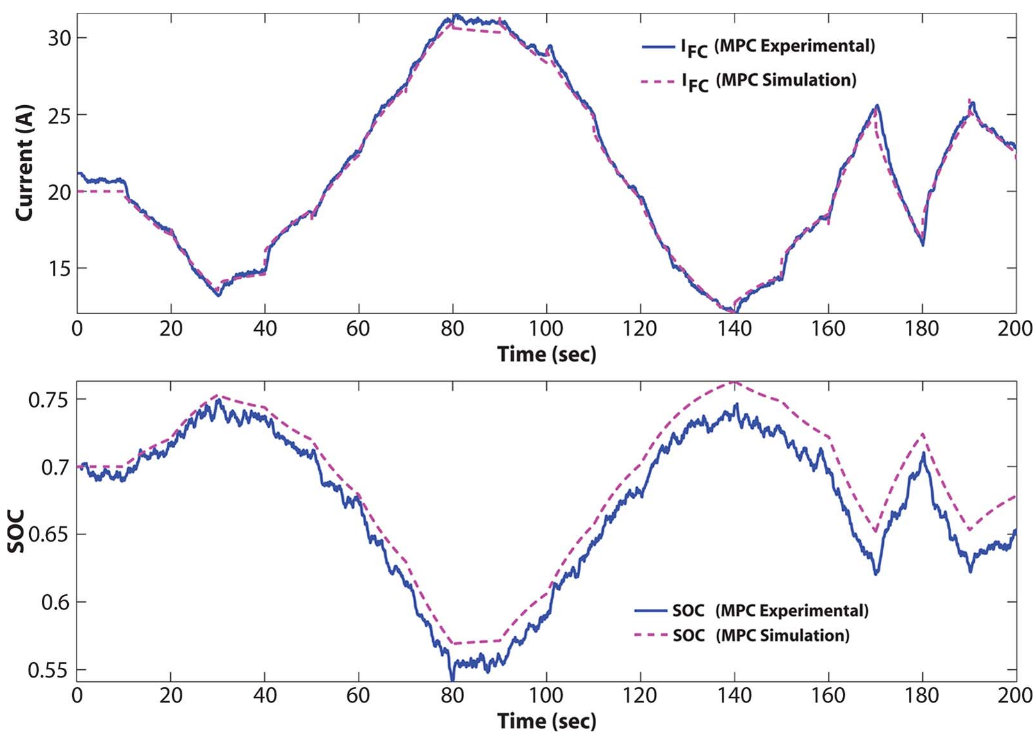

Fig. 8. Simulation versus experimental results: MPC.

A block diagram showing the structure of the MPC optimization process through a linear model is shown in Fig. 7. The MPC power management scheme was developed using the MPC toolbox in MATLAB and implemented using a dSPACE *ds*1003 controller board in test bench experiments. A sampling interval of 0.1 s was chosen. With this sampling interval, the computational time of solving the quadratic program did not pose a limit for the real-time implementation of the controller on the dSPACE target processor. Several papers have discussed the requirements for solving a quadratic program online in more details; see, for instance, [39].

IV. Experimental Results

A current demand profile which includes large transients and extended high and low power segments is used to test the performance of both rule-based and model predictive power management strategies. Figs. 8 and 9 show a comparison of the simulation and experimental results for both cases. The line resistance losses are relatively small but could have an influence on the experimental output. The bidirectional converter's nonlinear efficiency map could also be a source of error, as it was difficult to model accurately.

The performance of the rule-based controller was largely dependent on the control parameter settings. The tuning of the controller was achieved primarily by the adjustment of the filter time constant τ. This value determines how quickly the FC current approaches the demanded current. The final setting for τ was chosen to be 12.5 s through trial and error.

The tuning of the MPC strategy was more straightforward than the rule-based strategy, as the constraint on SOC could be explicitly enforced and the power split could be adjusted through the cost function weights. Table I lists the final penalty weights and constraints used in the MPC design. The prediction

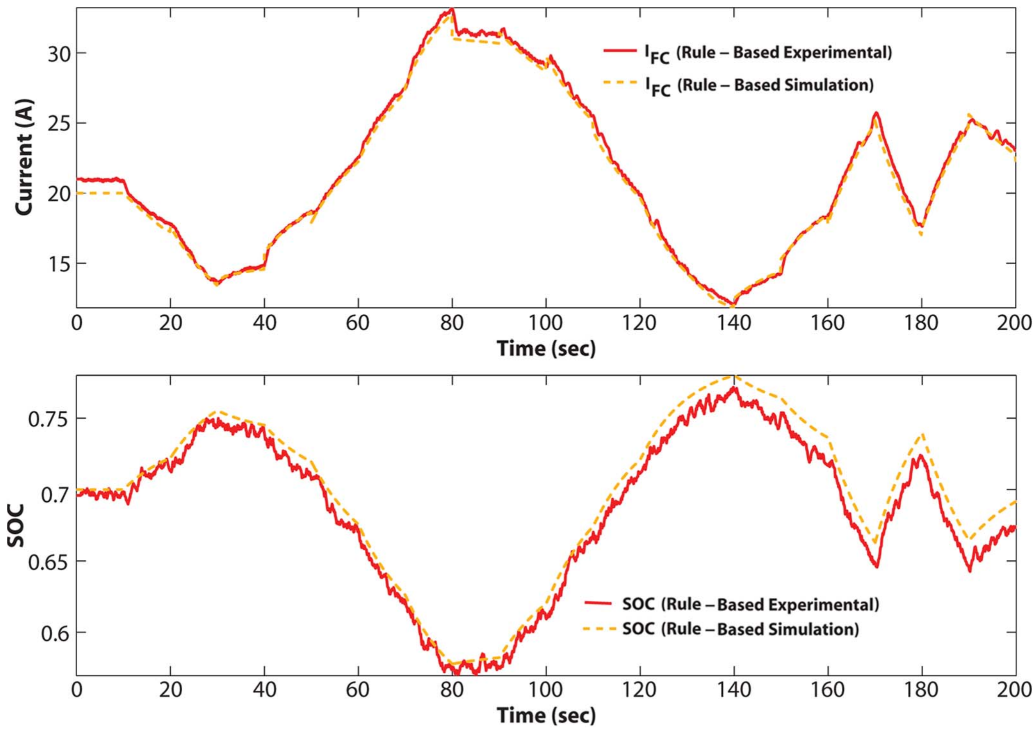

Fig. 9. Simulation versus experimental results: Rule-based control.

TABLE I
MPC CONSTRAINTS AND WEIGHTS

Parameter	Min	Max	Weight
SOC	0.5	0.9	550
I_{UC}	$-\infty$	∞	1

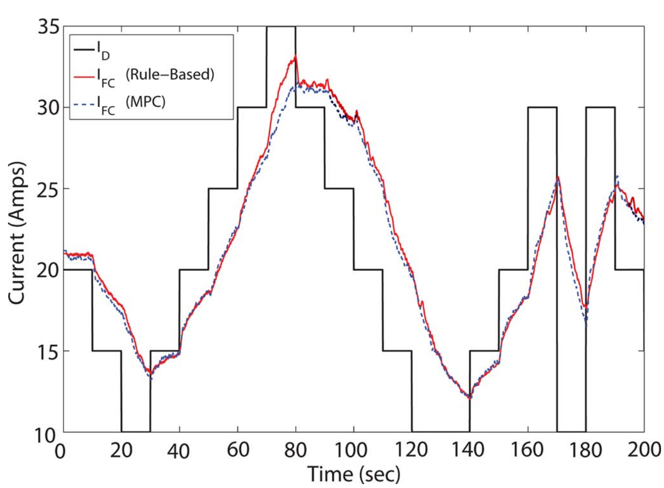

Fig. 10. MPC versus rule-based control: FC current comparison.

horizon P and control horizon N for the MPC controller were set to 20 and 2, respectively.

The controllers were tested in real-time under the same current demand profiles. Fig. 10 shows the FC current; the MPC controller's predictive nature results in smoother transitions in the current delivered by the FC.

Fig. 11 shows a comparison of how the UC bank was utilized by each controller. Both controllers absorbed the transients equally well until the SOC penalty effect limited the rule-based supply current.

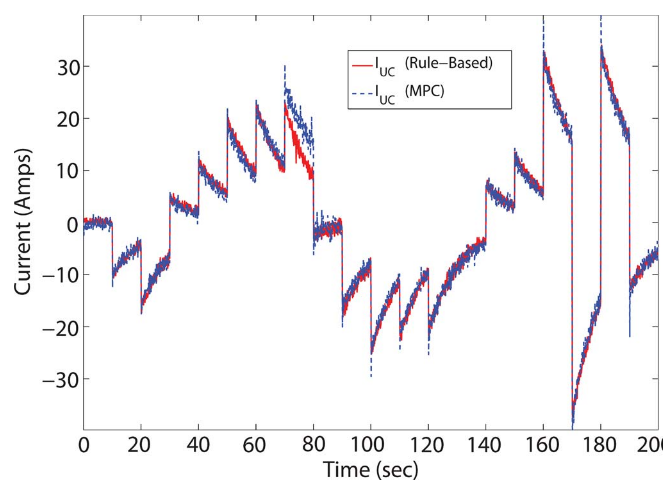

Fig. 11. MPC versus rule-based control: UC current comparison.

The rule-based controller was more conservative in using the UC bank to supply current, while the MPC controller was more aggressive. This can be easily seen in Fig. 12, where the MPC controller quickly approaches constraints without violating them (except for a very short period which may be due to the differences between the plant and the model). The rule-based controller could be tuned to act in a more aggressive manner, but this results in an abrupt decrease in the magnitude of UC current when a constraint is reached, leaving any other changes in loading to be absorbed by the FC.

The large current spikes in rule-based strategy occur when the SOC approaches its constraints. Fig. 13 shows the I_{FC} when the rule-based strategy assumes no limits on the UC SOC (uses $K = 1$). The plot compares this to the actual I_{FC} delivered (K determined using Fig. 6).

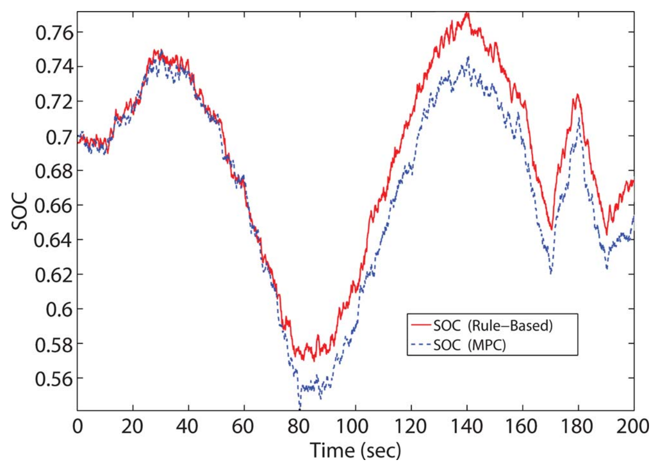

Fig. 12. MPC versus rule-based control: UC SOC comparison.

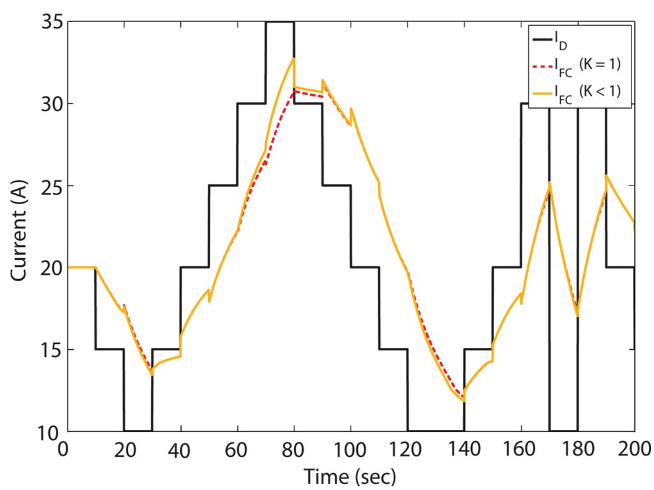

Fig. 13. SOC penalty effect: Rule-based control.

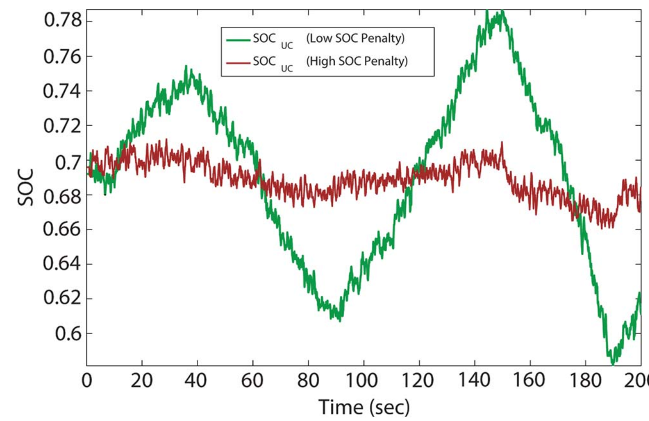

Fig. 14. SOC weighting effect.

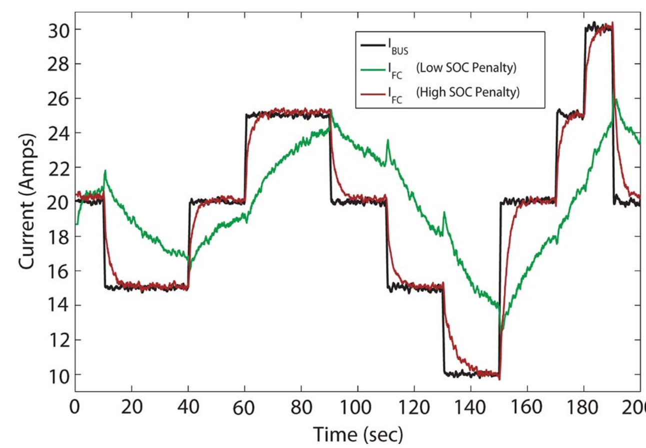

Fig. 15. SOC weighting effect: I_{UC} and I_{FC}.

The cost function, which is used to find the optimal control actions in MPC, can be adjusted to change the controller performance. The effect of changing the weights of the MPC controller is shown here through real-time results from the MPC controller. The two weights in the cost function are on the deviation from the requested UC current $(I_{\mathrm{UC}}^{\mathrm{OP}})$ and the deviation from the ideal SOC. The weight on I_{UC} was held constant, and the weight on SOC was varied to show the effects of different weighting. The low SOC penalty weighting was 400, and the high SOC penalty weighting was 1500. The relative weighting, not absolute weighting, is important in the MPC problem.

The effects of the large SOC penalty can be seen in Fig. 14. Such a large penalty on the SOC deviation results in very little use of the UC. The relative weighting can be adjusted for more aggressive or conservative performance, depending on the application.

Fig. 15 also shows the effect of a large SOC penalty has on the current split in the system. In the case of the large penalty, the UC bank is hardly used as a buffer, forcing the system to rely mainly on the FC to provide the demanded power.

Adjusting the prediction and control horizons is another method by which the performance of MPC controller can be tuned. Simulations were used to examine the effects of changes in these horizons. The MPC controller discussed previously was used for power management under a simple pulse current demand profile. The control horizon was maintained at a constant value of two, and weights were held constant.[1] The prediction horizon was adjusted from short to long, and the simulation results were recorded.

Fig. 16 shows the SOC of the UC under the various prediction horizons. From this plot, it can be seen that the UC bank is used in a more aggressive manner with a shorter prediction horizon. The reason for this may be that, with a longer prediction horizon, the anticipation of a SOC constraint violation results in a more conservative use of the UC bank and smaller deviations in SOC. Because of the wide variations in SOC under a small prediction horizon, the controller tends to perform poorly when reaching a constraint, but a long prediction horizon does not utilize the UC bank to its full advantage.

[1]The control horizon determines the number of unknown optimization variables (control moves) over the prediction horizon. Because the model predictive control problem is solved in a receding horizon manner and only the first of this control moves is really used and the other ones are recalculated at each sample time, large control horizons typically do not have a big influence on the results. They do increase the computational time significantly due to the increased size of the optimization problem. In the problem discussed in this paper, the results with control horizons larger than two are indistinguishable from each other and therefore difficult to see the difference in a plot. We only report the results with the control horizon of $N = 2$.

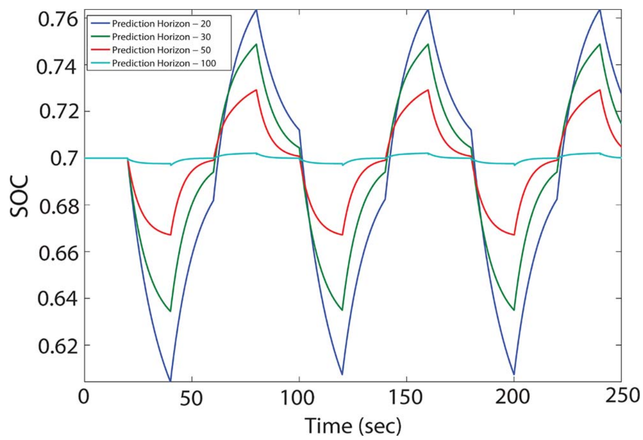

Fig. 16. SOC under varying prediction horizon.

The aforementioned experimental validation has been carried out with an electronic load which imposes dc current free of harmonics. Understanding the influence of switching harmonics on the performance of low- and high-level control systems has not been the focus of this paper and may be a good direction for future investigation.

V. Conclusion

The experimental results in this paper have shown the effectiveness of a two-degree-of-freedom control configuration for the power management of a UC–FC hybrid. A dc/dc converter in its current-control mode controlled the current taken from the FC and UC; another dc/dc converter in its voltage-control mode maintained a constant bus voltage. We have tested two current management strategies at the supervisory level: an optimization-based MPC algorithm and a rule-based algorithm that was tuned to do as well as the optimization-based approach. The feasibility of real-time implementation of both algorithms was shown in experiments. The MPC approach had the advantage of being easier to tune. Due to explicit handling of the UC SOC constraint in MPC, the UC bank can be used more aggressively to buffer sharp transients and supply power in times of high demand. The rule-based controller does not always fully utilize the power available from the UC bank. Moreover, the rule-based controller may need retuning if a different type of demand profile is expected while the optimization-based and predictive nature of MPC makes it applicable across a wider range of demand profiles. In addition, the MPC design process described in this paper can be carried out in more complex situations where the design of a rule-based algorithm is not intuitive. For example, when there are more than two power generation/storage sources, finding the optimal power balance is not straightforward with a rule-based algorithm. Moreover, if the dynamics of the FC are to be taken into account, resorting to model-based design may simplify the problem.

Acknowledgment

Publication of this paper in the IEEE Transactions on Industrial Electronics is with permission from the American Society of Mechanical Engineers.

References

[1] W. Gao, "Performance comparison of a fuel cell-battery hybrid powertrain and a fuel cell–ultracapacitor hybrid powertrain," *IEEE Trans. Veh. Technol.*, vol. 54, no. 3, pp. 846–855, May 2005.

[2] M. C. Kisacikoglu, M. Uzunoglu, and M. S. Alam, "Load sharing using fuzzy logic control in a fuel cell/ultracapacitor hybrid vehicle," *Int. J. Hydrogen Energy*, vol. 34, no. 3, pp. 1497–1507, Feb. 2009.

[3] M. E. Schenck, J. S. Lai, and K. Stanton, "Fuel cell and power conditioning system interactions," in *Proc. Appl. Power Electron. Conf. Expo.*, Mar. 2005, vol. 1, pp. 114–120.

[4] P. Thounthong, S. Rael, and B. Davat, "Test of a PEM fuel cell with low voltage static converter," *J. Power Sources*, vol. 153, no. 1, pp. 145–150, Jan. 2006.

[5] W. Schmittinger and A. Vahidi, "A review of the main parameters influencing long-term performance and durability of PEM fuel cells," *J. Power Sources*, vol. 180, no. 1, pp. 1–14, May 2008.

[6] J. M. Correa, F. A. Farret, L. N. Canha, and M. G. Simoes, "An electrochemical-based fuel-cell model suitable for electrical engineering automation approach," *IEEE Trans. Ind. Electron.*, vol. 51, no. 5, pp. 1103–1112, Oct. 2004.

[7] P. Rodatz, G. Paganelli, A. Sciarretta, and L. Guzzella, "Optimal power management of an experimental fuel cell/supercapacitor powered hybrid vehicle," *Control Eng. Pract.*, vol. 13, no. 1, pp. 41–53, Jan. 2005.

[8] Z. Jiang, L. Gao, M. J. Blackwelder, and R. A. Dougal, "Design and experimental tests of control strategies for active hybrid fuel cell/battery power sources," *J. Power Sources*, vol. 130, no. 1/2, pp. 163–171, May 2004.

[9] P. Thounthong, S. Rael, and B. Davat, "Control strategy of fuel cell/supercapacitors hybrid power sources for electric vehicle," *J. Power Sources*, vol. 158, no. 1, pp. 806–814, Jul. 2006.

[10] J. Bauman and M. Kazerani, "A comparative study of fuel-cell-battery, fuel-cell–ultracapacitor, and fuel-cell–battery–ultracapacitor vehicles," *IEEE Trans. Veh. Technol.*, vol. 57, no. 2, pp. 760–769, Mar. 2008.

[11] J. M. Miller, "Energy storage technology markets and applications: Ultracapacitors in combination with lithium-ion," in *Proc. 7th Int. Conf. Power Electron.*, Daegu, Korea, Oct. 2009.

[12] G. Zorpette, "Super charged," *IEEE Spectrum*, vol. 42, no. 1, pp. 32–37, Jan. 2005.

[13] M. Ortuzar, J. Moreno, and J. Dixon, "Ultracapacitor-based auxiliary energy system for an electric vehicle: Implementation and evaluation," *IEEE Trans. Ind. Electron.*, vol. 54, no. 4, pp. 2147–2156, Aug. 2007.

[14] W. Henson, "Optimal battery/ultracapacitor storage combination," *J. Power Sources*, vol. 179, no. 1, pp. 417–423, Apr. 2008.

[15] M. Garcia-Arregui, C. Turpin, and S. Astier, "Direct connection between a fuel cell and ultracapacitors," in *Proc. IEEE Int. Conf. Clean Elect. Power*, 2007, pp. 474–479.

[16] A. Emadi, K. Rajashekara, S. S. Williamson, and S. M. Lukic, "Topological overview of hybrid electric and fuel cell vehicular power system architectures and configurations," *IEEE Trans. Veh. Technol.*, vol. 54, no. 3, pp. 763–770, May 2005.

[17] Y. Jia, H. Wang, and M. Ouyang, "Electric power system for a Chinese fuel cell city bus," *J. Power Sources*, vol. 155, no. 2, pp. 319–324, Apr. 2006.

[18] D. Candusso, I. Valero, A. Walter, S. Bacha, E. Rulliere, and B. Raison, "Modelling, control and simulation of a fuel cell based power supply system with energy management," in *Proc. IEEE Annu. Conf. Ind. Electron. Soc.*, Nov. 2002, vol. 2, pp. 1294–1299.

[19] M. Uzunoglu and M. Alam, "Dynamic modeling, design, and simulation of a combined PEM fuel cell and ultracapacitor system for stand-alone residential applications," *IEEE Trans. Energy Convers.*, vol. 21, no. 3, pp. 767–775, Sep. 2006.

[20] P. Thounthong, S. Rael, and B. Davat, "Utilizing fuel cell and supercapacitors for automotive hybrid electrical system," in *Proc. IEEE Appl. Power Electron. Conf. Expo.*, Mar. 2005, vol. 1, pp. 90–96.

[21] A. Sciarretta, M. Back, and L. Guzzella, "Optimal control of parallel hybrid electric vehicles," *IEEE Trans. Control Syst. Technol.*, vol. 12, no. 3, pp. 352–363, May 2004.

[22] J. Moreno, M. Ortuzar, and J. Dixon, "Energy management system for a hybrid electric vehicle, using ultracapacitors and neural networks," *IEEE Trans. Ind. Electron.*, vol. 53, no. 2, pp. 614–623, Apr. 2006.

[23] C. Lin, H. Peng, J. Grizzle, and J. Kang, "Power management strategy for a parallel hybrid electric truck," *IEEE Trans. Control Syst. Technol.*, vol. 11, no. 6, pp. 839–849, Nov. 2003.

[24] A. Schell, H. Peng, D. Tran, E. Stamos, C. Lin, and M. Kim, "Modelling and control strategy development for fuel cell electric vehicles," *Annu. Rev. Control*, vol. 29, no. 1, pp. 159–168, Feb. 2005.

[25] A. Vahidi and W. Greenwell, "A decentralized model predictive control approach to power management of a fuel cell–ultracapacitor hybrid," in *Proc. Amer. Control Conf.*, 2007, pp. 5431–5437.

[26] A. Vahidi, A. Stefanopoulou, and H. Peng, "Current management in a hybrid fuel cell power system: A model predictive control approach," *IEEE Trans. Control Syst. Technol.*, vol. 14, no. 6, pp. 1047–1057, Nov. 2006.

[27] F. Barrero, M. R. Arahal, R. Gregor, S. Toral, and M. J. Duran, "A proof of concept study of predictive current control for VSI driven asymmetrical dual three-phase AC machines," *IEEE Trans. Ind. Electron.*, vol. 56, no. 6, pp. 1937–1954, Jun. 2009.

[28] S. Bolognani, S. Bolognani, L. Peretti, and M. Zigliotto, "Design and implementation of model predictive control for electrical motor drives," *IEEE Trans. Ind. Electron.*, vol. 56, no. 6, pp. 1925–1936, Jun. 2009.

[29] T. Geyer, G. Papafotiou, and M. Morari, "Model predictive direct torque control—Part I: Concept, algorithm and analysis," *IEEE Trans. Ind. Electron.*, vol. 56, no. 6, pp. 1894–1905, Jun. 2009.

[30] G. Papafotiou, J. Kley, K. G. Papadopoulos, P. Bohren, and M. Morari, "Model predictive direct torque control—Part II: Implementation and experimental evaluation," *IEEE Trans. Ind. Electron.*, vol. 56, no. 6, pp. 1906–1915, Jun. 2009.

[31] A. Becutti, S. Mariethoz, S. Cliquennois, S. Wang, and M. Morari, "Explicit model predictive control of dc–dc switch mode power supplies with extended Kalman filtering," *IEEE Trans. Ind. Electron.*, vol. 56, no. 6, pp. 1864–1874, Jun. 2009.

[32] P. Lezana, R. Aguilera, and D. Quevedo, "Model predictive control of an asymmetric flying capacitor converter," *IEEE Trans. Ind. Electron.*, vol. 56, no. 6, pp. 1839–1846, Jun. 2009.

[33] F. M. Oettmeier, J. Neely, S. Pekarek, R. DeCarlo, and K. Uthaichana, "MPC of switching in a boost converter using a hybrid state model with a sliding mode observer," *IEEE Trans. Ind. Electron.*, vol. 56, no. 9, pp. 3453–3466, Sep. 2009.

[34] P. Correa, J. Rodriguez, M. Rivera, and J. Espinoza, "Predictive control of an indirect matrix converter," *IEEE Trans. Ind. Electron.*, vol. 56, no. 6, pp. 1847–1853, Jun. 2009.

[35] S. Kouro, P. Cortes, R. Vargas, U. Ammann, and J. Rodriguez, "Model predictive control—A simple and powerful method to control power converters," *IEEE Trans. Ind. Electron.*, vol. 56, no. 6, pp. 1826–1838, Jun. 2009.

[36] J. M. Maciejowski, *Predictive Control With Constraints*. Englewood Cliffs, NJ: Prentice-Hall, 2002.

[37] M. M. Seron, G. C. Goodwin, and J. A. Dona, *Constrained Control and Estimation*. New York: Springer-Verlag, 2005.

[38] A. Bemporad, "Model predictive control design: New trends and tools," in *Proc. IEEE Conf. Decision Control*, 2006, pp. 6678–6683.

[39] A. Vahidi, I. V. Kolmanovsky, and A. Stefanopoulou, "Constraint management in fuel cells: A fast reference governor approach," in *Proc. Amer. Control Conf.*, 2005, pp. 834–839.

[40] W. Greenwell and A. Vahidi, "In predictive coordination of a fuel cell/ultracapacitor hybrid," in *Proc. ASME Dyn. Syst. Control Conf.*, 2008, pp. 119–126.

Wes Greenwell received the B.S. and M.S. degrees in mechanical engineering from Clemson University, Clemson, SC, in 2006 and 2008, respectively.

He is currently with Michelin Americas Research, Greenville, SC. His research interests include polymer electrolyte membrane fuel cells, power management in hybrid electric vehicles, automotive power electronics, and ultracapacitors as a power source for electric vehicles.

Ardalan Vahidi (M'07) received the B.S. and M.S. degrees in civil engineering from Sharif University, Tehran, Iran, in 1996 and 1998, respectively, the M.S. degree in transportation safety from The George Washington University, Washington, DC, in 2002, and the Ph.D. degree in mechanical engineering from the University of Michigan, Ann Arbor, in 2005.

He is currently an Assistant Professor of mechanical engineering with Clemson University, Clemson, SC. His current research interests are in optimization-based control methods and control of vehicular and energy systems.